

ARTICLE

# Understanding the Effect of Zinc Oxide (ZnO) With Carbon Black Coupling Agent on Physico-Mechanical Properties in Natural Rubber Matrix

Koushik Pal\*  Koushik Banerjee Soumya Ghosh Chowdhury Sanjay Kumar Bhattacharyya Rabindra Mukhopadhyay

Hari Shankar Singhania Elastomer and Tyre research Institute, Plot No. 437, Hebbal Industrial Area, Mysore, Karnataka, 570016, India

ARTICLE INFO

*Article history*

Received: 23 December 2022

Revised: 20 February 2023

Accepted: 21 February 2023

Published Online: 01 March 2023

*Keywords:*

Carbon black

Natural rubber

Carbon black coupling agent

Anti-reversion properties

ABSTRACT

Natural rubber (NR) is not only the main compounding ingredient used to make the majority of components of tires as well as other rubber products, as it plays a significant role in ensuring that they operate well and complies with environmental standards. The applications of NR products are limited to high temperatures due to the reversion tendency of NR vulcanizate. To address these issues, the potential engagement of a carbon black (CB) coupling agent (CA) in the presence of metal oxide i.e. Zinc Oxide (ZnO) was investigated in an NR-based system. This CA has dual functionality on physico-mechanical properties. CA has the ability to reduce hysteresis loss as well as improve anti-reversion properties and these properties thoroughly depend on the presence of ZnO. While ZnO was added to the master formulation, a 65% improvement in reversion properties was observed. On the other hand, while ZnO fully transferred to the final formulation, bound rubber (BR) content increased by 19%, the difference in storage modulus ( $\Delta G'$ ) is reduced by 22%, cure rate index (CRI) improved by 14%, loss tangent ( $\tan \delta$ ) reduced by 18% and slightly improve in elongation at break compared to control compound. Thermo-gravimetric analysis (TGA) was engaged to understand the thermal stability and degree of purity of CA. A differential Scanning Calorimeter (DSC) was used to detect the phase transition of CA. Fourier Transform Infrared Spectrum (FTIR) was adopted to detect the presence of carboxyl and amine groups in the CA moiety. Payne effect, BR content and Transmission Electron Microscope (TEM) were employed to investigate the micro-level dispersion of CB in the natural rubber (NR) matrix.

*\*Corresponding Author:*

Koushik Pal,

Hari Shankar Singhania Elastomer and Tyre research Institute, Plot No. 437, Hebbal Industrial Area, Mysore, Karnataka, 570016, India;

Email: [koushik.pal@jksmail.com](mailto:koushik.pal@jksmail.com); [pst.koushik@gmail.com](mailto:pst.koushik@gmail.com)

DOI: <https://doi.org/10.30564/opmr.v4i2.5341>

Copyright © 2022 by the author(s). Published by Bilingual Publishing Co. This is an open access article under the Creative Commons Attribution-NonCommercial 4.0 International (CC BY-NC 4.0) License. (<https://creativecommons.org/licenses/by-nc/4.0/>).

## 1. Introduction

There has been a huge demand to improve the fuel efficiency in passenger car tires as well as truck tires because of the increasing fuel price, greenhouse gas emission and implementation of government regulations on rolling resistance (RR) [1-6]. RR loss of a tire can be defined as the mechanical energy consumed when the tires roll over on the road surface for a unit distance [7,8]. RR is directly related to the loss tangent ( $\tan \delta$ ) of the compound. RR greatly enhances overall energy loss and has a direct impact on the fuel efficiency of a motor vehicle. As the rubbers are bad conductors of heat, there is an energy loss which leads to increased tire temperature during the running condition. The increase in temperature is effective on the reinforcement of the tire and ultimately its impact falls on the results as tread cuts and chips, treadwear and durability of the tire [4,9]. RR, mileage and durability are the three most considerable parameters for tire performance. So, there is a big challenge for researchers in this field to improve RR without compromising other properties.

A proper approach to the selection of rubber, chemicals and filler can significantly improve the tire properties [10]. Green compound properties can be improved through good dispersion of filler into the polymer matrix during mixing [11]. On the other hand, prolonged degradation of cured rubber can be achieved by using suitable anti-degradants. Generally, high structure and high surface area carbon blacks (CBs) are used in tire tread compound formulation to achieve better durability [12]. CB materials are aggregates of nanoparticles of spheroidal shape, typically 10-100 nm in diameter. The shape and degree of inter-linking of the aggregates are known as structure [13]. A "high structure" is characterized by extensive interlinking or branching, whereas a "low structure" is characterized by less pronounced interlinking or branching. In this experimental study, we used N134 CB, which has a particle size in the range of 11-19 nm. For this reason, the particles have a high tendency to form large aggregates of three-dimensional structure owing to their high surface area (the average surface area of N134 is 120-150 m<sup>2</sup>/gm). This high tendency to form large aggregates makes N134 CB into high-structure CB. It is difficult to mix this type of CB with rubber because of high shearing and heat generation during mixing. To overcome this, plasticizers and oils are included in the compound formulation. CBs and silica are the two most widely used fillers for tire tread formulation. It is well known that incorporation of silica in rubber matrix is very difficult because of its reverse polarity in comparison with most of the rubbers (rubber

is hydrophobic in nature and silica is hydrophilic) [14,15]. To address this, various silane coupling agents are used to create a bridging medium between rubber and silica. Similarly, to disperse CB into rubber moiety, using CB coupling agents (CA) came into the picture. Soumya et al. already discussed the potential of Sumilink 200, used as a CB CA for natural rubber tread compound formulation [16]. González et al. studied the influence of CB CA to improve the wet grip and RR of tires [17].

Heat generation in tire components also influences the aging rate of cured rubber compounds, and the effect of heat aging results in the polymer chain bond breakdown (softening) or conversion of Polysulfidic linkage to mono or di-sulfidic linkage (hardening), which mainly depends on the type of rubber and rubber chemicals used in rubber compound formulation [18,19]. This degradation of the rubber compound leads to a shorter service life of the tire. To achieve prolonged aging of the rubber compound, it is necessary to use the proper anti-aging chemical in the compound formulation.

In this study N'-methylidene-3-hydroxynaphthalene-2-carbohydrazide is used as a novel CA to improve CB dispersion. Its chemical structure is shown in Figure 1. Amine (-NH<sub>2</sub>) and hydroxyl (-OH) are the two different functional groups present in this chemical. The reactivity and functionality of this chemical enhances based on the presence of ZnO. In the absence of ZnO, CA fully functioned as a CB CA, while in the presence of ZnO it acts as a CB CA as well anti-reversion agent. There are few articles available, where researchers studied the influence of CB CA agents on rubber properties [18,20,21]. But, other than coupling efficiency, other properties evaluations for this type of chemical have been not yet done before. Our present study is carried out on an NR-CB-based system having CA and ZnO in the compounding formulation. In this study we are trying to investigate the reactivity on coupling efficiency of CA in absence of ZnO. On the other hand, we have split out ZnO dosage in the master and final recipe. The intention of this study is to find out the suitable dosage of ZnO and CA for obtaining the least heat generation as well as reversion.

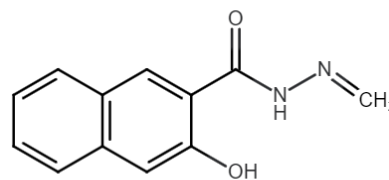


**Figure 1.** Molecular structure of N'-methylidene-3-hydroxynaphthalene-2-carbohydrazide.

## 2. Materials and Methods

### 2.1 Raw Materials

Natural rubber with grade SMR-20 (NR) was procured from Rubber Net (Asia) PTE Ltd., Indonesia and CA was supplied by Otsuka Chemical Private Ltd. (India). The other ingredients were used for this study as follows: N134 CB (Hi-tech Carbon Black Ltd, India), Zinc Oxide (ZnO) was supplied by POCL enterprises Ltd, Puducherry, India. The particle size of ZnO is in the range of 200 nm to 300 nm having an average particle size in the range of 250 nm. Stearic acid (VVF Ltd., India), Soluble sulfur (The Standard Chemical Co. Pvt Ltd.) and n-Cyclohexylbenzothiazol-2-sulphenamide (CBS) (Shandong Derek New Materials Co Ltd., Shandong, China).

### 2.2 Thermal Analysis

Thermo Gravimetric Analysis (TGA) of CA was performed by using Pyris-1 TG analyzer of Perkin-Elmer (Shelton, CT, USA) to understand the thermal degradation behavior of CA. This chemical was tested at a heating rate of 10 °C/min. The analysis was done by increasing the temperature from room temperature to 590 °C under a nitrogen atmosphere. During testing, the nitrogen atmosphere was used to create an inert atmosphere by preventing oxidative degradation.

To understand the reactivity of CA, Differential Scanning Calorimeter (DSC) with DSC 25 system (TA Instruments, Discovery series) was used. The analysis was done at a heating rate of 10 °C/min.

### 2.3 FTIR Study

Fourier Transform Infrared Spectroscopy (FTIR) of Perkin Elmer (Norwalk, CT, USA) was used to carry out micro-structure analysis of CA. The scanning range was from 500  $\text{cm}^{-1}$  to 4000  $\text{cm}^{-1}$  at a resolution of 4  $\text{cm}^{-1}$  to record the spectrum.

### 2.4 Preparation of Rubber Compound

All the compounds were mixed as per the formulation and corresponding mixing sequence mentioned in Table 1 and Table 2 respectively. The reaction between CA, NR and CB generally happened between 145-150 °C. So, during master batch mixing, we maintained this specific range of temperature for two minutes. The mixing for all the stages i.e. masters, repass and final was conducted in lab scale Banbury mixer (Stewart Boilling, USA). This Banbury was equipped with a two-wing rotor with a 1.6 L capacity. The temperature control unit (TCU) was maintained at 90 °C for master and repass and 70 °C for final

mixing.

**Table 1.** Detail formulation of the compounds.

Master					
Ingredients	Control	Exp 1	Exp 2	Exp 3	Exp 4
SMR20	100				
N134 Carbon Black	44				
Zinc Oxide	5	1	1.5	2.5	0
Stearic Acid	2				
CA	0	0.8			
Final					
Ingredients	Control	Exp 1	Exp 2	Exp 3	Exp 4
Zinc Oxide	0	4	3.5	2.5	5
Standard Sulphur	1.1				
CBS	1.7				

**Table 2.** Mixing sequence followed during Master, Repass and Final stage.

Time (sec)	Actions taken
MASTER Mixing Sequence	
0	Loading of the raw rubber and masticated for 30 sec at 50 rpm
30	Ram up and added carbon black and other chemical, ram down at 50 rpm
120	Ram sweep and ram down at 50 rpm
180	Ram sweep and ram down at 50 rpm
180-300	Maintain temperature at 145-150 °C
300	Ram up and discharge the batch
REPASS Mixing Sequence	
0	Load the master batch and ram down at 50 rpm
90	Ram sweep and ram down at 50 rpm
180	Ram up and batch discharge at 150 °C
FINAL Mixing Sequence	
0	Load the repass batch along with final chemicals and ram down at 30 rpm
90	Ram sweep and ram down at 30 rpm
180	Ram up and batch discharge

### 2.5 Cure Characteristics

The cure characteristic of the final compounds was measured by using P-MDR (model RPA 2000, Alpha technologies, Akron, OHIO, USA). From the rheometric curve minimum torque ( $M_L$ ), maximum torque ( $M_H$ ), scorch time ( $t_{s_2}$ ) and optimum cure time ( $t_{90}$ ) were generated. Where  $t_{s_2}$  corresponds to the time to rise 2-unit torque above the  $M_L$  value and  $t_{c_{90}}$  is the time required to achieve 90% of the  $M_H$  value.  $t_{c_{90}}$  of the compounds was deter-

mined by using Equation (1):

$$\text{Torque at 90\% cure} = 0.9 (M_H - M_L) + M_L \quad (1)$$

The cure rate index (CRI) stands for the rate of curing and was determined by the following Equation (2).

$$CRI = \frac{100}{(t_{c_{90}} - t_{s_2})} \text{min}^{-1} \quad (2)$$

The reversion of the compounds was calculated by using the following Equation (3).

$$\text{Reversion \%} = \frac{\text{Max Torque} - \text{Final Torque}}{\text{Max Torque}} \times 100 \quad (3)$$

## 2.6 Payne Effect

Dispersion of filler into rubber matrix was determined by Payne effect study. Shear storage modulus ( $G'$ ) at 1% to 100% strain at 50 °C and 1.67 Hz was measured by using Rubber Process analyzer (model RPA 2000, Alpha technologies, OHIO, USA). The difference in shear modulus at 0.1% and 100% ( $\Delta G'$ ) is known as Payne effect of the compound.  $\Delta G'$  values were calculated based on the following Equation (4).

$$\Delta G' = G' \text{ at 0.1\% strain} - G' \text{ at 100\% strain} \quad (4)$$

## 2.7 Bound Rubber Content

The solvent extraction process was used to determine the bound rubber (BR) content of the final compounds. 0.2-0.3 gm of rubber samples were duly packed inside a dried filter paper and keep it overnight in toluene solvent at 115-120 °C for extraction by using the Soxhlet apparatus. After complete extraction, the samples were kept in a hot air oven at 80 for one-two hours until they reached a constant weight. The total BRC percentage of the rubber compounds was calculated by using the following Equation (5) [22,23].

$$\text{Total BRC (\%)} = \frac{W_f - W \left( \frac{m_f}{m_f + m_p} \right)}{W \left( \frac{m_p}{m_f - m_p} \right)} \quad (5)$$

where  $W_f$ ,  $W$ ,  $m_f$  and  $m_p$  were denoted as final weight, initial weight, filler loading (%) and polymer loading (%) respectively.

## 2.8 Moulding

To prepare tensile slabs from the final compounds, moulding was performed (ASTM D3182) in an electrically heated hydraulic press (Hind hydraulics, India). The samples were cured at 145 °C for  $2t_{c_{90}}$  under 15 MPa pressure. To test the abrasion resistance of the compounds in the laboratory abrasion tester (LAT 100), samples were cured in a specially designed mould at 141 °C for 60 min under 15 MPa pressure. The dimension of the tensile

slab and LAT 100 samples were 0.15 m/0.15 m/0.002 m (length/width/thickness) and 0.08 m/0.035 m/0.18m (outer diameter/width/thickness) respectively.

## 2.9 Tensile Properties

Tensile properties from the cured slabs were measured according to ASTM D412 by using a universal testing machine (UTM, Z010, Zwick/Roell, Germany). The testing was conducted at a speed of 500 mm/min at room temperature. The various tensile properties like moduli at different percent elongation, tensile strength (TS) and elongation at break (EB) were generated from the tensile curve [24,25]. The hardness of the cured slabs was measured by a multi-unit hardness tester (MUHT) as per ASTM D2240.

## 2.10 Dynamic Mechanical Analysis (DMA)

Storage modulus, loss modulus and loss tangent ( $\tan \delta$ ) were measured by using a Dynamic mechanical analyzer (Model VA4000, manufactured by Metravib, France). Samples were prepared from cured slabs having a dimension of 10 mm/24 mm/2 mm (width/length/thickness) with a testing area of 10 mm. Samples were run at three specific temperatures (30 °C, 70 °C and 100 °C) at 5% strain with a frequency of 11 Hz.

## 2.11 TEM Images

Micro-level filler dispersion of reinforcing filler was captured by using high-resolution transmission electron microscopy (HRTEM), 200 kv Talos- S (FEI, Hillsboro, OR, USA). The samples were prepared by Ultra-microtomy (Leica Ultracut UCT) at -100 °C with a thickness of around 100 nm.

## 2.12 LAT 100 Testing

The abrasion resistance of the compounds was measured according to ISO/DIN 23233 by using Laboratory Abrasion Tester 100 (LAT 100, m/s VMI, Holland). The details testing configuration of this study are mentioned in the 3.9 LAT100 results section. The loss in mass of the test sample was measured and the loss per unit running distance was calculated as per Equation (6).

$$A = \frac{m}{s} \quad (6)$$

where,  $A$  is the loss in mass per unit running distance during the run, in mg/km;  $m$  is the loss in mass during the run, in mg; and  $s$  is the running distance, in km.

The wear rating was determined by comparing the loss in mass of the test sample per unit running distance with the loss in mass per unit running distance of the control

compound tested under the same condition. The rating of the tested compounds was assigned based on low, medium and high severity conditions as per the load speed and slip angles maintained during the testing. Based on the severity conditions, the average wear rating was estimated for the compounds.

### 3. Results and Discussion

#### 3.1 Material Characterization

Thermogravimetry (TG) and differential thermogravimetry (DTG) profile is presented in Figure 2(A). The curve shows a two-step degradation. Degradation at 331 °C and 630 °C indicate the molecular breakdown of CA. No volatile loss was observed within the temperature range of 90-180 °C. The characteristic peaks present in CA indicate the material is pure and free from other contaminants. From the TGA curve, it is clear that CA is thermally stable up to 331 °C and therefore can be mixed with rubber without thermal degradation.

DSC is a useful tool to get thermal safety-related information such as the heat of reaction ( $\Delta H$ ), exothermic onset temperature ( $T_o$ ) and a peak of temperature ( $T_p$ )<sup>[26]</sup>. Figure 2(B) depicts the calorimetric curve of CA. This clearly defines the fact that at around 150 °C, CA undergoes an intra molecular reaction. This may also be explained in a way that the activation energy corresponds to 150 °C, activates CA to become reactive. Thus, the improvement of any composite containing CA only shows improvement after

mixing which is around 150 °C.

The FTIR spectrum of CA is shown in Figure 2(C). Definite transmittance at 3409  $\text{cm}^{-1}$  is clearly evident in the presence of primary and secondary amine groups, whereas absorbance maxima at 1642  $\text{cm}^{-1}$  attributed to “-C=O” stretching of amide group presence in CA moiety<sup>[27]</sup>. The presence of such amide and carboxyl functional groups in CA is likely to create an environment for the interaction with the surface polar groups of CBs.

#### 3.2 Cure Characteristics

The effect of ZnO and CA on cure characteristics of NR-CB based compounds at 145 °C for 60 min is shown in Table 3. From the test results, it is observed that  $M_H$  value is the least and reversion percent is higher for Exp 4 compound compared to other variants. While the amount of ZnO (in phr) is gradually increased in a master batch of Exp 1, Exp 2 and Exp 3 compound formulation and it is observed that  $M_H$  value is much higher compared to Exp 4 compound. On the other hand, reversion percent also gradually decreases and it is the least for Exp 3 compound. This change can be explained based on the reaction mechanism, which is discussed in section 3.4. Due to the formation of a stable six-member ring between ZnO, hydroxyl group and amine group are present in CA, which improves the solubility and reactivity of ZnO. As a result, the formation of shorter sulfur crosslinks increases, which reflects in higher  $M_H$  value and lowering reversion percent against Exp 4 compound.

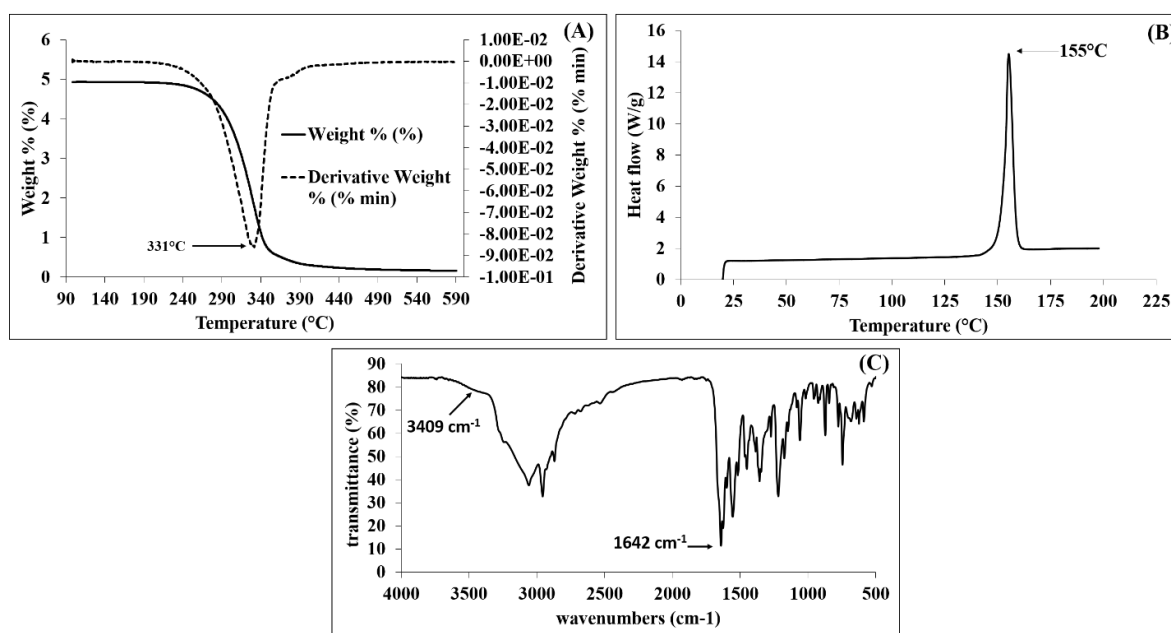


Figure 2. (A) TGA Curve, (B) DSC Curve, (C) FTIR Spectrum of CA.

Another interesting point that needs to be looked into is that the cure rate index (CRI) of Exp 4 compound is higher than others. This may be due to the presence of a higher amount of unreacted ZnO in the final batch for Exp 4 compound. A larger number of ZnO can react with the accelerator to generate an active Zn-accelerator complex which then accelerate the vulcanization reaction.

**Table 3.** Rheometric properties of all the formulations at 145 °C/60 min.

Rheometric Properties	Control	Exp 1	Exp 2	Exp 3	Exp 4
$M_L$ (dNm)	2.98	3.54	3.59	3.42	3.38
$M_H$ (dNm)	18.89	19.75	19.53	19.29	16.72
$M_H-M_L$ (dNm)	15.91	16.22	15.93	15.87	13.35
$ts_2$ (min)	10.37	9.41	9.58	9.69	9.63
$tc_{40}$ (min)	12.10	10.60	10.77	10.82	10.60
$tc_{90}$ (min)	17.07	16.35	16.88	16.79	15.51
final torque (dNm)	18.49	19.56	19.35	19.14	16.36
% Reversion	2.15	0.97	0.93	0.76	2.16
CRI	14.93	14.41	13.70	14.08	17.01

### 3.3 Reaction Mechanism

As we have already mentioned that CA has a dual-functioning ability; it acts as a coupling agent as well as an anti-reversion agent. The coupling activity is plausible because of the presence of two reactive sites in the CA moiety, hydrazide group and pi-electron cloud of the naphthalene group. During mixing, due to shear force, active radicals are formed in NR chains which then react with the hydrazide group of CA. On the other hand, pi-electron of naphthalene group physically reacts with functional

groups present in the CB. In this way, CA shows the coupling reactivity with NR and CB. The reaction mechanism is presented in Figure 3(A).

CA is also functioning as an anti-reversion agent due to the presence of ZnO in the reaction medium. The hydroxyl groups and amine groups present in CA form a stable six-member ring with ZnO, which results in increasing the solubility and reactivity in the rubber matrix. Higher ZnO reactivity results in the formation of shorter sulfur crosslinks, which improves compounds' thermal properties also. After the formation of this ZnO complex, CA has less opportunity to react with NR for the NR-CB coupling effect. A details reaction mechanism is shown in Figure 3(B).

### 3.4 Bound Rubber (BR)

BR gives an idea about the rubber-filler interaction in the uncured state. Physical and chemical interactions are supposed to involve during BR formation. In this matter of CB dispersion, free radical interaction between the filler surface groups and the polymer is proposed as a mechanism for BR formation<sup>[16]</sup>. The BR content of the uncured compounds is shown in Figure 4. It is observed that BR content is higher for Exp 4 compound. This result suggests that the interaction between rubber-filler improves in absence of ZnO. It is also observed that there is a gradual decrement of BR content value from Exp 1 to Exp 3 compound. This is because of the gradually increased ZnO phr in the formulation. Presence of ZnO leads to a lowering affinity of CA on CB dispersion. These trends of results are strongly supported by the Payne effect values, which are discussed in section 3.5.

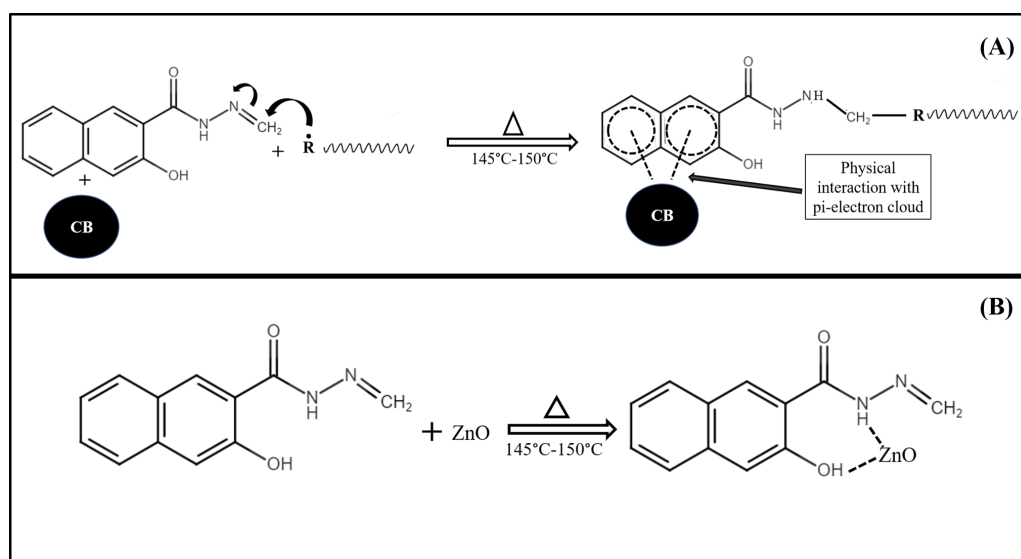


**Figure 3.** (A) and (B) reaction mechanism between Natural rubber, CA and ZnO.

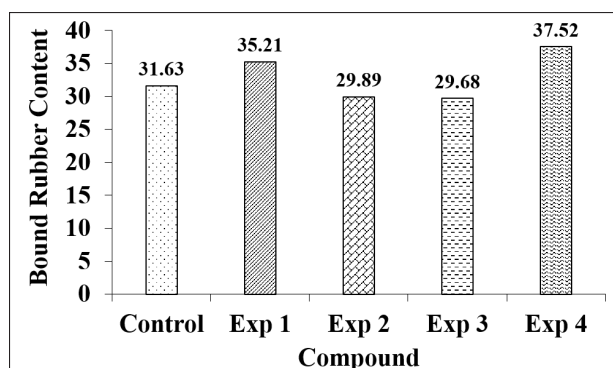


Figure 4. Bound rubber of the compounds.

### 3.5 Payne Effect

Payne effect of the green compounds is shown in Figures 5(A) and 5(B). From the results it is clear that inclusion of ZnO in final formulation reduces the Payne effect as compared to ZnO added in the master formulation. The gradual increase in Payne effect value from Exp 1 to Exp 3 confirms the less dispersion of filler in the polymer matrix. For Exp 4 compound, a lower  $\Delta G'$  value implies better CB dispersion compare to control compound.

### 3.6 Physical Properties

Mechanical properties of the control and the experimental compounds are shown in Table 4. It was observed that there was a marginal drop in high strain modulus (M200, M300) in the experimental compounds. The TS and EB remained unaltered. In fact, there was a decent improvement found in elongation properties of the experimental compounds. Exp 4 showed the best combination of properties among the variants tested. From the results, it was evident that the addition of CA did not deteriorate the mechanical properties of the compounds; rather it improved the EB and toughness. The combination of tensile strength and EB leads to materials of high toughness<sup>[28,29]</sup>. EB and toughness are the two fundamental reinforcing

properties of a rubber compound. When ZnO was used completely in the final batch (i.e. Exp 4), it was able to react chemically with CA in a more effective way such that the best properties were obtained in the compound. Exp 4 compound exhibit a higher toughness value, which actually indicates better dispersion of filler. This improvement in filler dispersion strongly correlates with BR and Payne effect values, which are discussed in section 3.4 and section 3.5 respectively. However, it has to be observed under dynamic conditions how CA would affect the compound properties.

Table 4. Physical properties at 145 °C/2 $t_{c90}$ .

Physicals Properties	Control	Exp 1	Exp 2	Exp 3	Exp 4
M100 (MPa)	2.3	2.2	2.3	2.3	2.2
M200 (MPa)	6.7	6.0	6.3	6.2	6.3
M300 (MPa)	13.6	12.4	12.7	12.5	13.0
Tensile Strength (MPa)	29.6	29.4	29.2	29	30.2
Elongation at Break (%)	513	537	530	522	530
Hardness (Shore A)	60	61	61	61	59
Toughness (J/m <sup>3</sup> )	15185	15788	15476	15138	16006

### 3.7 DMA Results

The visco-elastic properties of the rubber compounds are mentioned in Table 5. It has been noticed that  $\tan \delta$  decreases progressively with a comparable dynamic stiffness value ( $E'$ ) while total ZnO is transferred to the final formulation. It is already proven that  $\tan \delta$  of rubber compound is basically controlled by inter-aggregate distance between filler particles<sup>[30]</sup>. As the CA has the potential to disperse CB in absence of ZnO, so it is also evident from the test results that the lowering of  $\tan \delta$  is mainly because of CA activity. While ZnO was used in the master stage, there were not many changes observed in  $\tan \delta$ . Still there is an increment of  $E'$  value. The presence of reactive ZnO leads to formation sorter sulfur crosslink and results in higher  $E'$  value.

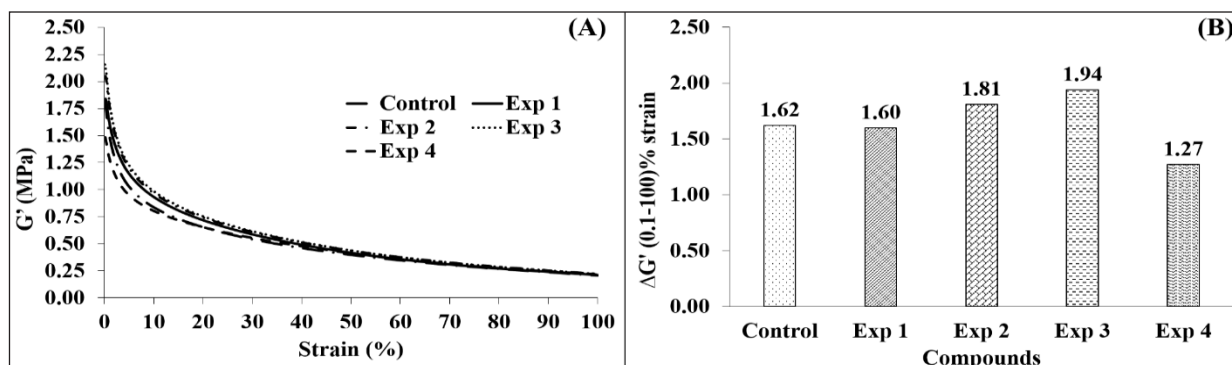


Figure 5. (A) Graphical representation of Payne Effect, (B) Payne effect represent by Bar Chart.

**Table 5.** Dynamic mechanical properties.

DMA at 5% strain, 11 Hz					
DMA at 30 °C	Control	Exp 1	Exp 2	Exp 3	Exp 4
E' (MPa)	7.25	7.51	7.89	7.68	6.5
E'' (MPa)	1.27	1.30	1.43	1.35	0.93
tan delta (tan $\delta$ )	0.175	0.173	0.181	0.175	0.143
DMA at 70 °C	Control	Exp 1	Exp 2	Exp 3	Exp 4
E' (MPa)	5.94	6.27	6.50	6.38	5.67
E'' (MPa)	0.87	0.93	1.02	0.96	0.69
tan delta (tan $\delta$ )	0.147	0.148	0.157	0.151	0.121
DMA at 100 °C	Control	Exp 1	Exp 2	Exp 3	Exp 4
E' (MPa)	4.92	5.28	5.40	5.31	4.89
E'' (MPa)	0.65	0.72	0.79	0.74	0.54
tan delta (tan $\delta$ )	0.131	0.137	0.146	0.140	0.11

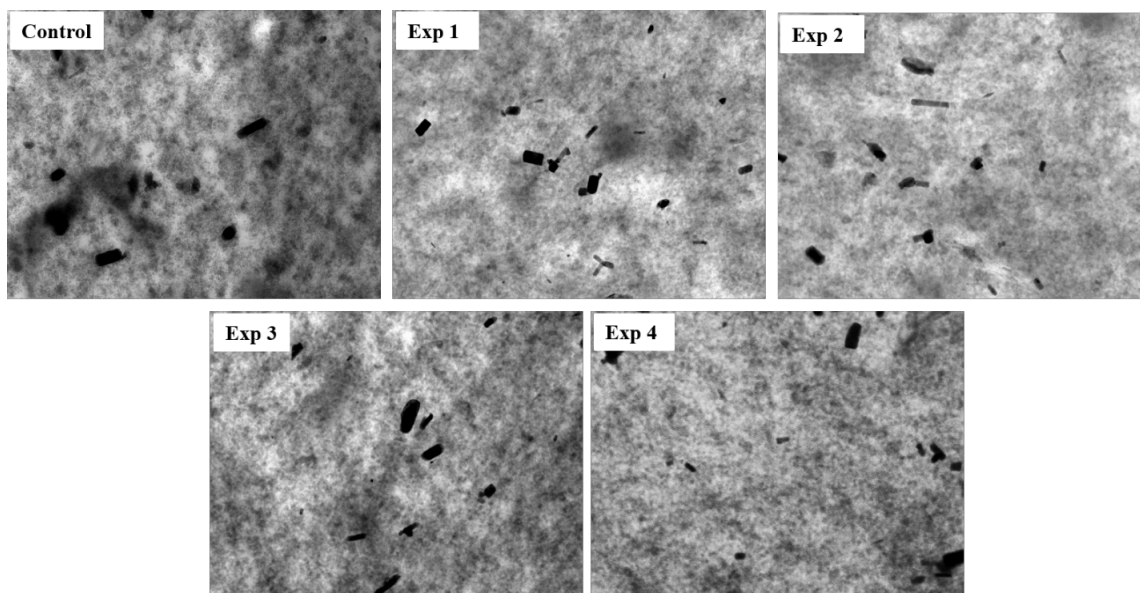
### 3.8 TEM Images

One of the most important parts of this study is to determine the micro-level dispersion of CB in a natural rubber matrix. TEM is a very useful tool for microscopic analysis to understand the degree of dispersion and orientation of the filler in higher magnification. Microscopic images were captured at 1100 $\times$  magnification by TEM from the cured slabs and it is represented in Figure 6. From the TEM images, it is seen that for Exp 4 compound, CB is good distributed throughout the rubber matrix. This observation is also correlating with the Payne effect results, i.e. the lowering of  $\Delta G'$  in Exp 4 compound owing to well dispersion of CB, which is discussed in section 3.6.

With addition of ZnO in master formulation (i.e. for Exp 1, Exp 2 and Exp 3 compounds), leads to relatively lower CB dispersion while comprising with Exp 4 compound. Agglomeration of CB is clearly visible in rubber matrix in Exp 1, Exp 2 and Exp 3 compounds.

### 3.9 LAT100 Results

The abrasion resistance rating of the experimental compound Exp 4 against the control was presented in Table 6. One of the targets of this study is to find out a plausible compound formulation where the compound will have the lowering hysteresis loss with a comparable abrasion loss. Exp 4 compound was chosen against control because of the lower hysteresis value in Exp 4 compound among other variants. As per the average ratings, Exp 4 exhibited a better wear rating (103) than the control (100) compound across severities. This signifies that, CA was not only instrumental in lowering the hysteresis of the compound, but also improved the wear properties. This might be due to the chemical interaction of CA with the surface functional groups present in carbon black as discussed in the mechanism section, thereby, forming the chemical bonds, which are much more stable than the conventional physical bonds that were created during the reinforcement of carbon black compounds. As a consequence of stronger chemical bonds, CA has provided better reinforcement in the experimental compound (Exp 4) as compared to the control. The enhanced wear characteristic of Exp 4 reflected its improved reinforcement.

**Figure 6.** TEM images (comparison at 1100 $\times$  magnification).



**Table 6.** LAT 100 test configuration and results.

Abrasion loss test condition			Wear rating	
Load (Newton)	Speed (km/hour)	Slip angle (°)	Control	Exp 4
75	25	16	100	94
		9	100	99
		5.5	100	90
	12	16	100	101
		9	100	113
		5.5	100	111
	2.5	16	100	108
		9	100	97
		5.5	100	112
Average rating*			100	103

\*higher the ratings better the abrasion resistance.

#### 4. Conclusions

This study unveils the great potential of the Carbon Black (CB) coupling agent in the natural rubber carbon black system. While ZnO is added to the master formulation, CA acts as an anti-reversion agent and for Exp 3 compound shows a 65% improvement in reversion compared to the control compound. On the other hand, while ZnO fully transferred to the final formulation, Bound rubber (BR) content increased by 19%, the difference in storage modulus ( $\Delta G'$ ) is reduced by 22%, CRI improved by 14% and slightly improve in elongation at break compare to control compound. Bound rubber content, Payne effect and microscopic study through TEM have substantiated the potential of the CA on CB dispersity in absence of ZnO from the master formulation. In addition to that hysteresis loss is lowered by 18% with comparable dynamic stiffness ( $E'$ ) at 70 °C compare to the control compound. Abrasion loss was measured to assess the potential of CA in practical application. Abrasion resistance is slightly improved in Exp 4 compound when compared with the control compound. Overall, it was observed that CB CA can act as an anti-reversion agent as well carbon black coupling agent depending on the presence of the ZnO in the compound formulation.

#### Author Contributions

Koushik Pal: Conceptualization, methodology, compound mixing, data generation, investigation, writing -original drift.

Koushik Banerjee: Compound mixing, compound level

testing, data generation, writing - review.

Soumya Ghosh Chowdhury: Formal analysis, investigation, writing - review.

Sanjay Kumar Bhattacharyya: Conceptualization, resources, review and editing supervision.

Rabindra Mukhopadhyay: Conceptualization, resources, review and editing, supervision.

#### Conflict of Interest

The authors declared no potential conflicts of interest with respect to the research, authorship, and/or publication of this research article.

#### Acknowledgements

All authors would like to thank “Hari Shankar Singhanian Elastomer and Tire Research Institute” management for giving kind permission to publish this research article.

#### References

- [1] Dong, B., Liu, C., Lu, Y., et al., 2016. Effects of hybrid filler networks of carbon nanotubes and carbon black on fracture resistance of styrene-butadiene rubber composites. *Polymer Engineering and Science*. 56, 1425-1431.  
DOI: <https://doi.org/https://doi.org/10.1002/pen.24379>
- [2] Byers, J.T., 2002. Fillers for balancing passenger tire tread properties. *Rubber Chemistry and Technology*. 75, 527-548.  
DOI: <https://doi.org/10.5254/1.3547681>
- [3] Bhawal, P., Das, T.K., Ganguly, S., et al., 2019. Selective cross-linking of carboxylated acrylonitrile butadiene rubber and study of their technological compatibility with poly(ethylene-co-methyl acrylate) by means of mechanical, thermal, and chemical analysis. *Polymer Bulletin*. 76, 1877-1897.  
DOI: <https://doi.org/10.1007/s00289-018-2474-z>
- [4] Zhang, P., Morris, M., Doshi, D., 2016. Materials development for lowering rolling resistance of tires. *Rubber Chemistry and Technology*. 89, 79-116.  
DOI: <https://doi.org/10.5254/rct.16.83805>
- [5] Das, T.K., Bhawal, P., Ganguly, S., et al., 2019. Synthesis of hydroxyapatite nanorods and its use as a nanoreinforcement block for ethylene methacrylate copolymer matrix. *Polymer Bulletin*. 76, 3621-3642.  
DOI: <https://doi.org/10.1007/s00289-018-2565-x>
- [6] Urreaga, J.M., Matias, M.C., De la Orden, M.U., et al., 2000. Effects of coupling agents on the oxidation and darkening of cellulosic materials used as reinforcements for thermoplastic matrices in composites. *Polymer Engineering and Science*. 40, 407-417.

- DOI: <https://doi.org/10.1002/pen.11174>
- [7] Hess, W.M., Klamp, W.R., 1983. Effects of carbon black and other compounding variables on tire rolling resistance and traction. *Rubber Chemistry and Technology*. 56, 390-417.  
DOI: <https://doi.org/10.5254/1.3538134>
- [8] Hall, D.E., Moreland, J.C., 2001. Fundamentals of rolling resistance. *Rubber Chemistry and Technology*. 74, 525-539.  
DOI: <https://doi.org/10.5254/1.3547650>
- [9] Bhattacharya, A.B., Pandey, M., Naskar, K., 2021. Development of NR/SBR based rubber compounds with low hysteresis and high durability for transmission v-belts applications. *Organic Polymer Material Research*. 3, 5.  
DOI: <https://doi.org/10.30564/opmr.v3i1.3568>
- [10] Das, T.K., Ghosh, P., Das, N.C., 2019. Preparation, development, outcomes, and application versatility of carbon fiber-based polymer composites: a review. *Advanced Composite and Hybrid Material*. 2, 214-233.  
DOI: <https://doi.org/10.1007/s42114-018-0072-z>
- [11] Pandey, J.K., Singh, R.P., 2005. Green nanocomposites from renewable resources: Effect of plasticizer on the structure and material properties of clay-filled starch. *Starch/Staerke*. 57, 8-15.  
DOI: <https://doi.org/10.1002/star.200400313>
- [12] Zafarmehrabian, R., Gangali, S.T., Ghoreishy, M.H.R., et al., 2012. The effects of silica/carbon black ratio on the dynamic properties of the tread compounds in truck tires. *E-Journal of Chemistry*. 9, 1102-1112.  
DOI: <https://doi.org/10.1155/2012/571957>
- [13] Khodabakhshi, S., Fulvio, P.F., Andreoli, E., 2020. Carbon black reborn: Structure and chemistry for renewable energy harnessing. *Carbon*. 162, 604-649.  
DOI: <https://doi.org/10.1016/j.carbon.2020.02.058>
- [14] Choi, S.S., Kim, J.C., Ko, J.E., et al., 2007. Influence of coupling agent on properties of carbon black-reinforced SBR and NR/SBR vulcanizates. *Journal of Industrial and Engineering Chemistry*. 13, 1017-1022.
- [15] Sattayanurak, S., Sahakaro, K., Kaewsakul, W., et al., 2020. Synergistic effect by high specific surface area carbon black as secondary filler in silica reinforced natural rubber tire tread compounds. *Polymer Testing*. 81, 106173.  
DOI: <https://doi.org/10.1016/j.polymertesting.2019.106173>
- [16] Chowdhury, S.G., Pal, K., Satpathi, H., et al., 2020. Improving hysteresis of a typical carbon black-filled natural rubber tread compound by using a novel coupling agent. *Progress in Rubber, Plastic and Recycling Technology*. 36, 245-261.  
DOI: <https://doi.org/10.1177/1477760619895015>
- [17] González, L., Rodríguez, A., de Benito, J.L., et al., 1996. A new carbon black-rubber coupling agent to improve wet grip and rolling resistance of tires. *Rubber Chemistry and Technology*. 69, 266-272.  
DOI: <https://doi.org/10.5254/1.3538371>
- [18] Stoček, R., Kratina, O., Ghosh, P., et al., 2017. Influence of thermal ageing process on the crack propagation of rubber used for tire application. *Springer Series in Materials Science*. 247, 351-364.  
DOI: [https://doi.org/10.1007/978-3-319-41879-7\\_24](https://doi.org/10.1007/978-3-319-41879-7_24)
- [19] Jitkarnka, S., Chusaksri, B., Supaphol, P., et al., 2007. Influences of thermal aging on properties and pyrolysis products of tire tread compound. *Journal of Analytical and Applied Pyrolysis*. 80, 269-276.  
DOI: <https://doi.org/10.1016/j.jaap.2006.07.008>
- [20] Choi, S.S., 2006. Influence of polymer-filler interactions on retraction behaviors of natural rubber vulcanizates reinforced with silica and carbon black. *Journal of Applied Polymer Science*. 99, 691-696.  
DOI: <https://doi.org/10.1002/app.22562>
- [21] Han, S., Kim, W.S., Mun, D.Y., et al., 2020. Effect of coupling agents on the vulcanizate structure of carbon black filled natural rubber. *Composite Interfaces*. 27, 355-370.  
DOI: <https://doi.org/10.1080/09276440.2019.1637197>
- [22] Qian, S., Huang, J., Guo, W., et al., 2007. Investigation of carbon black network in natural rubber with different bound rubber contents. *Journal of Macromolecular Science, Part B Physics*. 46(B), 453-466.  
DOI: <https://doi.org/10.1080/00222340701257588>
- [23] Wolff, S., Wang, M.J., Tan, E.H., 1993. Filler-elastomer interactions. Part VII. Study on bound rubber. *Rubber Chemistry and Technology*. 66, 163-177.  
DOI: <https://doi.org/10.5254/1.3538304>
- [24] Kiliçarslan, Ş., Türker, Y.Ş., 2020. Investigation of wooden beam behaviors reinforced with fiber reinforced polymers. *Organic Polymer Material Research*. 2, 1-7.  
DOI: <https://doi.org/10.30564/opmr.v2i1.1783>
- [25] Maurya, S.D., Singh, M.K., Amanulla, S., et al., 2022. Mechanical, electrical and thermal properties of nylon-66/flyash composites: Effect of flyash. *Organic Polymer Material Research*. 4, 7-14.  
DOI: <https://doi.org/10.30564/opmr.v4i2.5233>
- [26] Huang, S.T., Duh, Y.S., Hsieh, T.Y., et al., 2012. Thermal analysis for nano powders of iron and zinc by DSC. *Procedia Engineering*. 45, 518-522.  
DOI: <https://doi.org/10.1016/j.proeng.2012.08.196>

- [27] Milani, G., Milani, F., 2012. Comprehensive numerical model for the interpretation of cross-linking with peroxides and sulfur: Chemical mechanisms and optimal vulcanization of real items. *Rubber Chemistry and Technology*. 85, 590-628.  
DOI: <https://doi.org/10.5254/rct.12.88945>
- [28] Hassan, M.M., Wagner, M.H., Hayder, U., 2012. Study on the performance of hybrid jute / betel nut fiber reinforced polypropylene composites. *Journal of Adhesive Science and Technology*. 25, 615-626.  
DOI: <https://doi.org/10.1163/016942410X525858>
- [29] Hassan, M.M., Wagner, M.H., Zaman, H.U., et al., 2010. Physico-mechanical performance of hybrid betel nut (Areca catechu) short fiber/seaweed polypropylene composite. *Journal of Natural Fibers*. 7, 165-177.  
DOI: <https://doi.org/10.1080/15440478.2010.504394>
- [30] Pal, K., Chowdhury, S.G., Mondal, D., et al., 2021. Impact of  $\alpha$ -cellulose as a green filler on physico-mechanical properties of a solution grade styrene-butadiene rubber based tire-tread compound. *Polymer Engineering and Science*. 61, 3017-3028.  
DOI: <https://doi.org/10.1002/pen.25814>